SUPPRESSION EFFECT OF NICKEL FOAM ON THE EXPLOSION OF METHANE/ETHANE MIXTURE

by

Dongping YANG[a*], Yulong DUAN[b,c*], Min GUO[a], Weibin WANG[a], and Yang LIU[a]

[a] SINOPEC Shengli Oilfield Technical Testing Center, Dongying, China
[b] College of Safety Engineering,
Chongqing University of Science and Technology, Chongqing, China
[c] Chongqing Key Laboratory for Oil and Gas Production Safety and Risk Control Technology,
Chongqing, China

Original scientific paper
https://doi.org/10.2298/TSCI240907267Y

Methane (CH_4) and ethane (C_2H_6) are the main components of natural gas and coal bed gas in some regions of China, and the presence of ethane further exacerbates the risk of explosions, posing significant safety challenges during the production, storage, transportation, and use of natural gas. This study utilizes an self-constructed small-size experimental platform to investigate the suppression effect of nickel foam on the explosion of CH_4/C_2H_6 mixture in explosion tubes. The results show that nickel foam has two different effects on the CH_4/C_2H_6 flame: promotion and suppression. When the explosion flame quenching fails, the explosion is more violent, the flame propagation velocity and the peak explosion overpressure are both increased, and the peak velocity, the peak pressure, appear at the second wave. When the explosion flame quenching successfully, the flame propagation velocity peak and the explosion overpressure peak are attenuated, and the velocity peak and pressure peak appear in the first wave. The 40PPI nickel foam has the best effect on CH_4/C_2H_6 mixture explosion suppression.

Key words: *CH_4/C_2H_6, Ni foam, explosive characteristics, suppression*

Introduction

With the development of the economy and the adjustment of the global energy structure, gas fuel has become increasingly widely used for its high heat energy, low pollution, and low cost [1]. Natural gas consists mainly of CH_4, C_2H_6, and other small amounts of alkanes [2]. Also, coal bed gas in some areas appears as wet gas with 5%-43% heavy hydrocarbon content, of which the C_2H_6 component accounts for more than 90% of the total heavy hydrocarbon gas [3]. The presence of C_2H_6 can increase the risk of explosions, causing significant safety challenges during the production, storage, transportation, and use of natural gas.

The CH_4 and C_2H_6 as the major components of natural gas, associated oilfield gas, and *wet coal bed gas*. The uncertainty of explosion hazards caused by CH_4/C_2H_6 mixture attracts many scholars to study it. Su *et al.* [4] investigated the relationship between flame emission spectra and explosion characteristics of CH_4/C_2H_6/air mixtures, they found that in the fuel-poor state, P_{max} and $(dP/dt)_{max}$ increase with C_2H_6, while the time to reach P_{max} decreases with C_2H_6.

* Corresponding authors, e-mail: 3894857371@qq.com, 14924928@qq.com

It has been confirmed that the more hydrocarbons such as C_2H_6 account for in the natural gas composition, the flame propagation speed, peak explosion pressure, and maximum rate of pressure rise increase gradually [5]. Therefore, research on explosion isolation and suppression technologies to reduce the explosion hazards of CH_4/C_2H_6 mixtures is very important to ensure the safe production and transportation of explosive gas.

The main suppression methods of gas explosion are porous media [6], inert gases [7], fine water mists [8], and solid powders [9]. Among them, porous materials are widely used in explosion suppression [10] because of their unique pore structure and environmental protection, high hardness, high temperature resistance, strong resistance to sintering, and other advantages [11]. Currently, studies on the effect of porous materials on gas explosion suppression mainly focus on the research areas of CH_4 and CH_4/H_2 mixtures. However, little research has been done on suppressing CH_4/C_2H_6 mixture explosions by porous materials. Therefore, it is essential to study the influence of porous materials on the explosive characteristics of CH_4/C_2H_6 gas and to reveal their intrinsic mechanisms that promote or inhibit the explosive behavior of CH_4/C_2H_6 gas.

The unique pore structure of porous materials can effectively inhibit explosion overpressure and quench the flame [12]. When the explosion shock wave and explosion flame pass through the porous material, the pressure wave will be reflected at different angles due to the porous material's structure [13, 14], the collision chances of the active radicals in the explosion and combustion reactions with the inner wall of the porous pores increase dramatically, and many free radicals lose their activity. Thus achieving the purpose of reducing the peak explosion overpressure and flame temperature and accelerating the flame quenching. If quenching fails, the porous material acts as an obstacle to accelerate flame propagation [15], resulting in more serious consequences. Long *et al.* [16] found that 20 PPI porous material failes to quench a low hydrogen CH_4 explosion flame and escalated the explosion. However, 40 PPI porous material can quench the flame successfully. Wu [17] shows that 10 PPI porous material promotes the explosion flame, and 30 PPI porous material is very easy to promote the flame to form a localized explosion due to the large blocking ratio, resulting in failure suppression. Other studies have shown that the failure of explosion suppression in porous materials may also depend on the properties of the combustible gas itself. Zhou *et al.* [18] found that mesh Al alloy and Al velvet can suppress CH_4/C_2H_6 mixture gas explosions, but promote H_2/air and C_2H_2/air mixture gas explosions in their experiments.

In conclusion, most of the current research has focused on investigating the suppression effect of porous materials on single gas or analyzing the explosion characteristics of CH_4/C_2H_6 gas mixtures only. However, little research has been done on the effect of porous materials on the explosion suppression of CH_4/C_2H_6 mixtures. In this paper, widely used porous materials with different porosities of 30 PPI and 40 PPI was selected to study the explosion characteristics of a CH_4/C_2H_6 mixture with C_2H_6 volume fractions of 10%, 20%, and 30%, respectively, and explore the suppression effect of porous materials on the CH_4/C_2H_6 explosion. The relevant research results can provide data support and theoretical basis for the explosion prevention and suppression of natural gas and its associated gas, petroleum gas, coalbed CH_4, *etc.* during extraction and transportation.

Experimental set-up

Experimental platform construction

As shown in fig. 1, the experimental platform used in this study mainly consists of an experimental bench, an explosion experimental pipe, a gas distribution system, an ignition

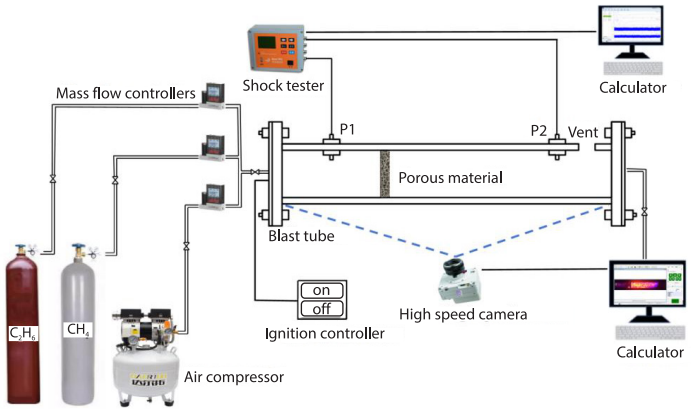

Figure 1. Diagram of the experimental set-up

system, a flame image acquisition system, and a pressure acquisition system. The explosion experiment pipe-line consists of 100 mm × 100 mm × 1000 mm square pipe and porous foam nickel composition. The square pipe can withstand the internal pressure of 2 MPa, and the pipe wall thickness is 20 mm. Both ends of the pipe are closed with a thickness of 10 mm steel plate with silicone pads. The left side of the steel plate is reserved for ventilation and ignition head installation port, and the right side of the steel plate is reserved for the exhaust port, in the pipe-line at the top of the tail to take the diameter of 3 cm of the explosion relief port. In all experiments, the vents were covered and sealed with PVC film. The gas distribution system consisted of CH_4 gas cylinders, C_2H_6 gas cylinders, air gas cylinders, and three mass-flow meters. The CH_4 and C_2H_6 were 99.99% pure, ambient air was used for the air, and the mass-flow meter was a high sensitivity mass-flow control meter from Alicat (range 0-5 Lpm, meter error ±0.4% of reading). The experiments were carried out at an equivalence ratio of 1.0 and a mixture of 10% ~ 30% C_2H_2. Calculate the gas-flow ratio parameters:

$$\varphi = \frac{\dfrac{n_{\text{fuel}}}{n_{\text{air}}}}{\left(\dfrac{n_{\text{fuel}}}{n_{\text{air}}}\right)_{\text{stopic}}} \tag{1}$$

$$\varphi = \frac{\dfrac{n_{C_2H_6}}{n_{C_2H_6}}}{\dfrac{n_{CH_4}}{}} \times 100\% \tag{2}$$

A 4-fold volume gas distribution method was used to ensure that the remaining gas in the pipe-line was discharged [19]. By calculating the volume of the relevant pipe-line and reading the flow meter, we estimate that the time required to fill the pipe-line at ambient temperature and pressure entirely is approximately 2 minutes. In addition, the exhaust system located on the right side of the pipe-line can effectively exhaust all gases in the exhaust pipe-line, thereby promoting the air replacement process inside the pipe-line, which involves using a mixture of air and fuel to replace the original air in the pipe-line [20]. This inflation phase is expected to last for 8 minutes.

The ignition system comprises a homemade ignition head, a high frequency pulse igniter, an ignition controller, and an ignition power supply (4 batteries). The power supply

input voltage is 6 V. Two platinum wires with a diameter of 0.1 mm are welded at the ignition position produce a high temperature spark. The flame image acquisition system comprises a PhantomV710L high speed camera and PCC graphics processing software. The camera is set at 1280 × 240 pixels and shoots at 2000 fps. The pressure acquisition system comprises two pressure sensors and a data acquisition module. Pressure Sensor 1 (from now on referred to as P1) is installed at a distance of 17.5 cm from the ignition head, and pressure Sensor 2 (from now on referred to as P2) is installed at a distance of 77.5 cm from the ignition head, pressure sensors pick up signals of pressure changes at both ends of the porous material. The pressure sensor has a range of 0-690 kPa and a linearity error of less than 1%.

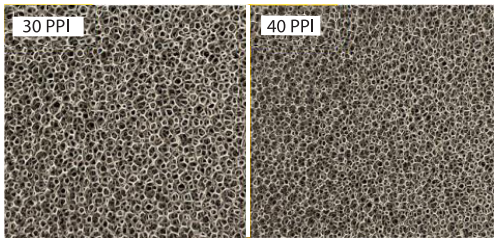

Figure 2. Porous material-nickel foam

Experimental methods and working conditions

As shown in fig. 2, two types of nickel foam with different porosity were selected for the porous material, and the pore density unit PPI (pores per linear inch) was 30 and 40, respectively. The nickel foam cross-section size is 100 × 100 mm^2 with a thickness of 10 mm, and the nickel foam is mounted in a fixed position (300 mm from the ignition end). To ensure the accuracy of the experiments, each of the nine sets of experimental conditions shown in tab. 1 was repeated 3-4 times.

Table 1. Experimental conditions

Serial number	C2H6 volume fraction, φ [%]	Porosity of porous materials [PPI]
C1	10	–
C2	20	–
C3	30	–
C4	10	30
C5	20	30
C6	30	30
C7	10	40
C8	20	40
C9	30	40

Analysis of experimental results

Flame structure changes

Hu *et al.* [21] found in 1996 that the combustion propagation process of combustible gases in pipe-lines can be divided into four stages, *i.e.*, the spherical flame stage, the finger flame stage, the flat flame stage, and the tulip flame stage. Figure 3 shows the dynamic propagation process of the CH_4/C_2H_6 mixture explosion flame in an empty pipe. As shown in fig. 3, the flame propagation process in all three concentrations is from spherical to finger to plane to *tulip* shape, and finally, the flame is transmitted to the end of the pipe, and the combustion reaction is completed and extinguished. For example, in fig. 3(a), when the C_2H_6 volume fraction φ = 10%, the structural change of the CH_4/C_2H_6 mixture explosion flame front

went through four stages: spherical flame (t = 15 ms), finger flame (t = 35 ms), plane flame (t = 50 ms), and tulip flame (t = 66.5 ms).

Comparison of figs. 3(a)-3(c) can be seen. The empty pipe selected C_2H_6 volume fractions of 10%, 20%, and 30%, respectively, to carry out experimental studies on the CH_4/C_2H_6 mixture of the evolution of the flame front structure of the explosion does not have a significant difference, have gone through the aforementioned four stages. With increasing volume fraction of C_2H_6, the explosion process of premixed gases is more rapid and violent [22]. As shown in fig. 3(b) at 46.50 ms and fig. 3(c) at 48.5 ms, the planar-shaped structure of figs. 3(b) and 3(c) reaches faster compared to that of fig. 3(a) at 50 ms.

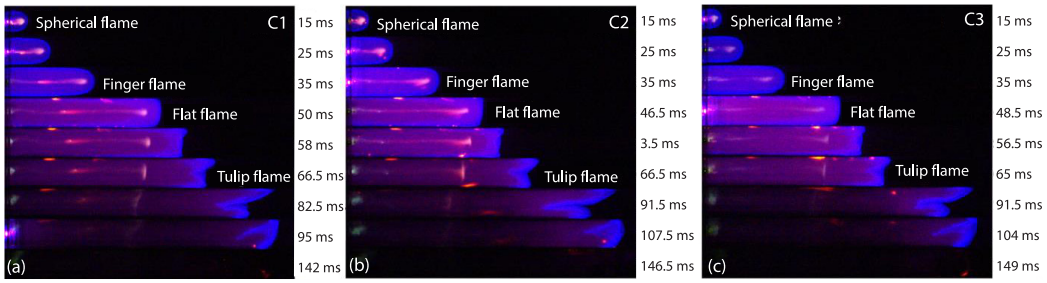

Figure 3. Dynamic flame propagation process of CH_4/C_2H_6 mixture explosion in an empty pipe; (a) φ = 10%, (b) φ = 20% and (c) φ = 30% (*for color image see journal web site*)

When there is porous material in the explosion experiment pipe-line, the propagation process of premixed CH_4/C_2H_6 gas explosion flame is effected by porous material with different porosity, the flame structure between the conditions appears apparent differences, and with the increase of C_2H_6 proportion in the premixed gas, the degree of flame variation becomes greater [4].

Figure 4 shows the effect of nickel foam with a porosity of 30 PPI on the dynamic flame propagation process of CH_4/C_2H_6 mixture explosion. Figure 4(a) shows that the flame failed to penetrate the porous material when the volume fraction of C_2H_6 is 10%, and the porosity of the porous material is 30 PPI. However, in figs. 4(b) and 4(c), increasing the proportion of C_2H_6 in the premixed CH_4/C_2H_6 gas, the premixed combustion reaction becomes more intense, the porous material fails to block the flame, flame penetrates the porous materials, as shown in fig. 4(b) at t = 67.5 ms and fig. 4(c) at t = 61 ms. The flame passes through the porous material and ignites the downstream explosive mixture gas, and the flame rapidly fills the pipe, spreading irregularly from left to right. The center of the flame shows a chaotic and disorderly state, and the color is bright yellow. Flame front laminar flow combustion is destroyed, turbulence is

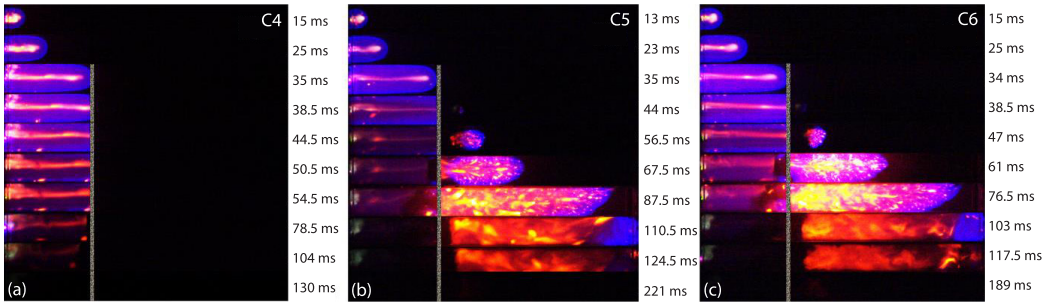

Figure 4. Effect of nickel foam (30 PPI) on flame propagation in methane/ethane mixture explosion; (a) φ = 10%, (b) φ = 20%, and (c) φ = 30% (*for color image see journal web site*)

increased, and the color is light blue. The whole process of propagation no longer appears as a *tulip* flame structure. Accelerated propagation above the flame front toward the vent. When the solid phase structure of foam nickel cannot extinguish the flame through its energy absorption, it may cause secondary deflagration. This is because the flame will be split into many small jet flames when passing through the porous micro-channels, and the limited energy absorption capacity of foam nickel has a limited effect on these small flames. These small flames propagate downstream along the porous material, igniting the unburned gas and leading to detonation. In this process, porous materials can be seen as a mesh-like obstacle, which not only blocks the propagation path of some flames but also promotes the transition from laminar flames to turbulent flames, thereby intensifying the intensity of the explosion.

Figure 5 shows the effect of nickel foam with a porosity of 40 PPI on the dynamic flame propagation process of a CH_4/C_2H_6 mixture explosion. Figure 5 is different from fig. 4 in that when the nickel foam porosity is 40 PPI, the increase in porosity further increases the number of tiny channels inside the nickel foam. Thus, flame propagation is blocked and quenched, and the flame fails to penetrate the porous material. As can be seen from fig. 5, after the premixed gas is ignited and propagates along the pipe to the pressure relief port, the flame structure evolves from hemispherical to finger-shaped, and in the transition from finger-shaped to plane-shaped, the flame front contacts the nickel foam and then enters into the interior of the nickel foam. Because of the existence of a certain number of disordered pore structures within the nickel foam, at this time, the flame edge contacts the pipe-line wall, and the flame front is in the deceleration stage. Therefore, the flame energy entering the porous interior is gradually converted and absorbed, and the flame is cooled and quenched.

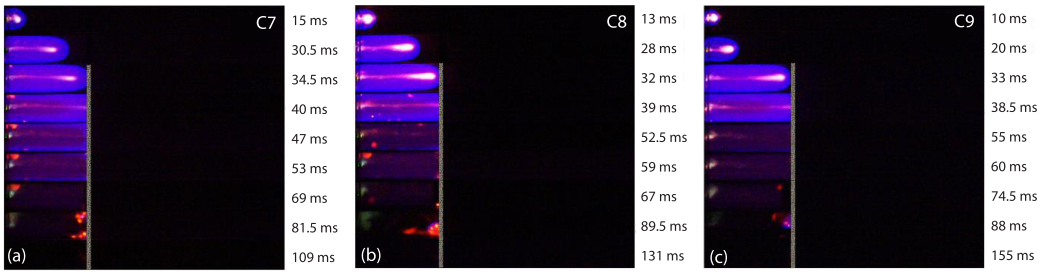

Figure 5. Effect of nickel foam (40 PPI) on flame propagation in CH_4/C_2H_6 mixture explosion; (a) φ = 10% (b) φ = 20%, and (c) φ = 30% (*for color image see journal web site*)

Comparison of figs. 4 and 5 can be found when the nickel foam porosity of 30 PPI, the explosion flame propagation appeared to produce quenching success or quenching failure of the two effects, when the volume fraction of C_2H_6 is 10%, nickel foam successfully quenched the flame, while the volume fraction of C_2H_6 is 20% and 30%, quenching failure occurs, and the flame intensifies, resulting in a secondary explosion phenomenon. The explosion flame is successfully quenched when the nickel foam porosity is 40 PPI.

Flame front velocity

The flame front velocity in the pipe depends on the flame propagation distance and the corresponding time interval Δt. The flame propagation distance is determined by the position of the leading edge of the flame front (L_1, L_2) corresponding to the two-time points (t_1, t_2). Flame velocity equation:

$$v = \frac{\Delta L}{\Delta t} = \frac{L_2 - L_1}{t_2 - t_1} \tag{3}$$

Figure 6 shows the flame propagation velocity of CH_4/C_2H_6 mixture explosion in an empty pipe-line. It can be seen that the overall trend of the explosion flame propagation velocity in the pipe-line increases first and then decreases, reaches the peak at about 30 cm from the ignition source. The peak flame velocity is 17.61 m/s when φ = 10%, 17.70 m/s when φ = 20%, and 18.24 m/s when φ = 30%. As can be seen from fig. 6, the empty pipe selected different volume fractions of C_2H_6 to carry out experimental studies. The CH_4/C_2H_6 mixture explosion flame propagation velocity trend is not significantly different, and, with the increase of the volume fraction of C_2H_6 increases, the explosion reaction of CH_4/C_2H_6 mixture increases, and the flame propagation speed accelerates.

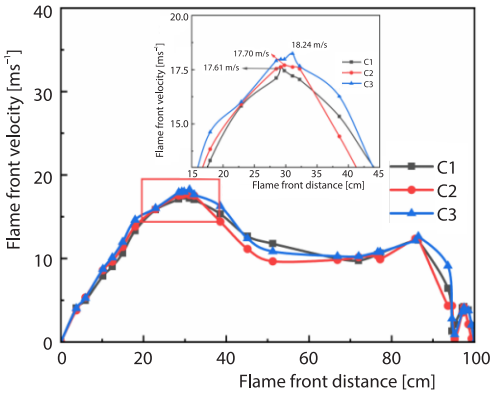

Figure 6. Flame propagation velocity of CH_4/C_2H_6 mixture explosion in an empty pipe

Figure 7 shows the relationship between flame propagation speed and flame front distance of CH_4/C_2H_6 mixed gas explosion with foam nickel of different porosity. The gray rectangular portion of fig. 7 indicates flame propagation up to 30 cm (installation position of nickel foam). It can be seen that the flame velocity only peaks once when the nickel foam successfully quenches the CH_4/C_2H_6 mixture explosion flame. If the flame quenching fails, the propagation process will be accelerated twice, with the first acceleration occurring near 30 cm and the second acceleration occurring near 70 cm to get the second peak velocity. Moreover, the explosive reaction intensifies after flame quenching fails, and the flame may be converted to detonation to a certain extent. Hence, the flame propagation rate increases dramatically after the failure of quenching. Fluctuations in the flame propagation speed curve were observed at the pressure relief port at the end of the pipe-line. This phenomenon occurs because when the front of the explosion flame reaches the pressure relief port, the flame will be stretched, increasing the speed of flame propagation. When the flame passes through the pressure relief port, the stretching effect weakens, thus forming a similar peak. As shown in fig. 7, when the quenching effect of foam nickel fails, the flame speed curve fluctuates in the gray area. This is because when the flame passes through foam nickel, it is quenched by the cold wall of porous materials, resulting in the temperature drop of the explosion flame, and the propagation speed also decreases. However, once the flame passes through foam nickel, this cold wall quenching effect will no longer work, rapidly increasing flame speed.

As shown in fig. 7, when φ = 10%, because the volume fraction of C_2H_6 in the CH_4/C_2H_6 gas mixture accounts for a relatively small percentage, the flame is quenched by 30 PPI and 40 PPI nickel foam, and no secondary acceleration phenomenon occurs. When φ = 20% and the porosity of nickel foam is 30 PPI, a secondary acceleration phenomenon occurs after the flame penetrates the nickel foam, and the peak flame velocity accelerates from 14.88-17.06 m/s. When φ = 30%, similar to fig. 7(b) when the nickel foam porosity is 30 PPI, the flame also shows a secondary acceleration phenomenon, and the peak velocity of the secondary acceleration is 19.54 m/s. When the nickel foam porosity is 30 PPI, quenching is successful only when the C_2H_6 volume fraction is 10%, and quenching fails when the C_2H_6 volume fraction is 20% and 30%. The CH_4/C_2H_6 mixture explosion flames is quenched successfully when the nickel foam porosity is 40 PPI. As shown in fig. 7, in the presence of nickel foam in the explosive

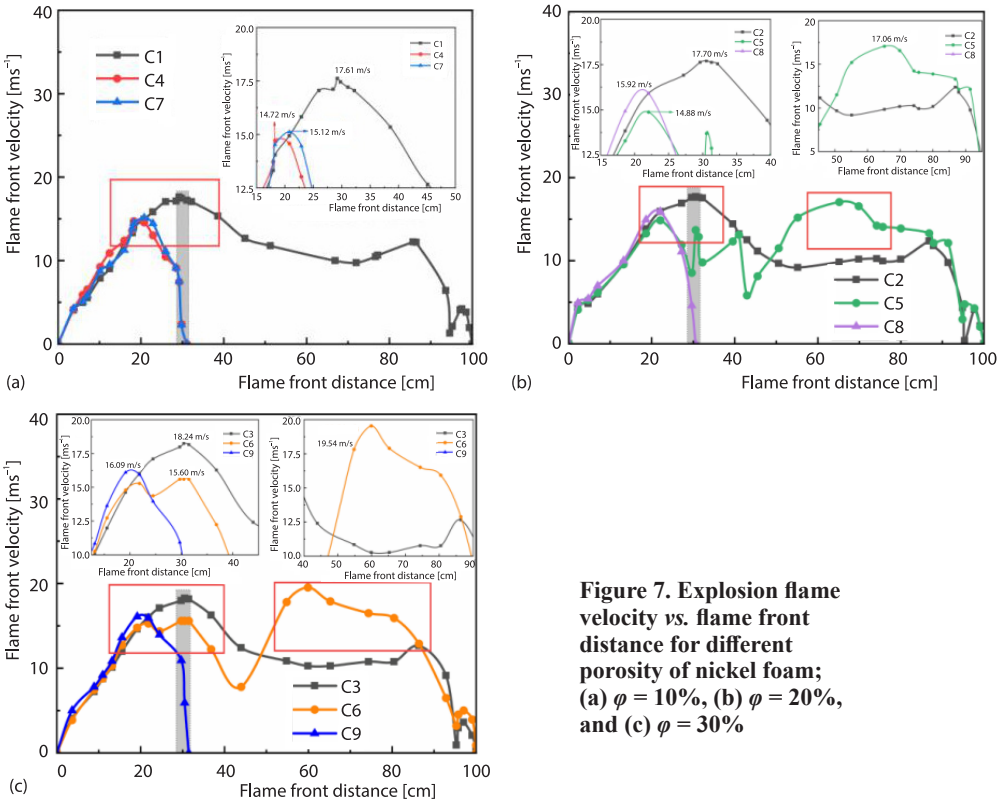

Figure 7. Explosion flame velocity *vs.* flame front distance for different porosity of nickel foam; (a) φ = 10%, (b) φ = 20%, and (c) φ = 30%

pipe-line, the explosion propagation velocity increases with the increase of the volume fraction of C_2H_6. Compares fig. 7 with fig. 6, the flame propagation velocity is significantly affected when the nickel foam. When quenching is successful, the flame propagation velocity tends to increase and then decrease. When the quench fails, the flame propagation shows two peaks, and the flame speed after passing through the nickel foam is more rapid than the flame speed at the same distance in fig. 6.

In summary, the analysis shows that nickel foam and volume fraction of C_2H_6 affect the velocity of the flame front of the CH_4/C_2H_6 mixture explosion. The addition of C_2H_6 increases the flame front speed [22]. Nickel foam promotes or inhibits flame front velocity depending on its porosity. When the nickel foam porosity is 30 PPI, the CH_4/C_2H_6 mixture explosion has two scenarios: quenching successful or quenching failure. When the C_2H_6 volume fraction is 10%, quenching successful, the flame front velocity only has one peak, when the C_2H_6 volume fraction is 20% and 30%, quenching failure, the flame front velocity only has two peaks, the second peaks is more remarkable compared to the first one. The second acceleration after the flame quenching failure will promote the flame front, so that the explosion is more violent. When the nickel foam porosity is 40 PPI, the CH_4/C_2H_6 mixture explosion is quenched successfully, and there is only one peak in the flame front velocity, *i.e.*, the flame propagation is accelerated only once.

Explosion overpressure

Figure 8 shows the dynamic explosion overpressure of CH_4/C_2H_6 explosion in empty pipe, fig. 8(a) shows the upstream explosion overpressure P1, and fig. 8(b) shows the down-

stream explosion overpressure P2. The figure shows that as the peak explosion overpressure increase with the increase of C_2H_6 fraction, indicating that the volume fraction of C_2H_6 is positively correlated with the explosion overpressure. In addition, due to the PVC membrane rupture, secondary deflagration, and other factors, the explosion overpressure curve shows multi-peak characteristics. The pressure sensor inside the pipe-line records subtle changes during the flame acceleration process. After the overpressure generated by the explosion reached its highest value, significant fluctuations were observed. This phenomenon can be attributed to the reflection of shock waves by the surrounding environment during flame propagation, which propagates in the form of transverse waves in front of the flame, leading to pressure oscillations. Radulescu *et al.* [23] captured the release of transverse waves inside the pipe-line. They compared it with the pressure oscillation data recorded in the experiment, explaining the pressure oscillation inside the pipe-line.

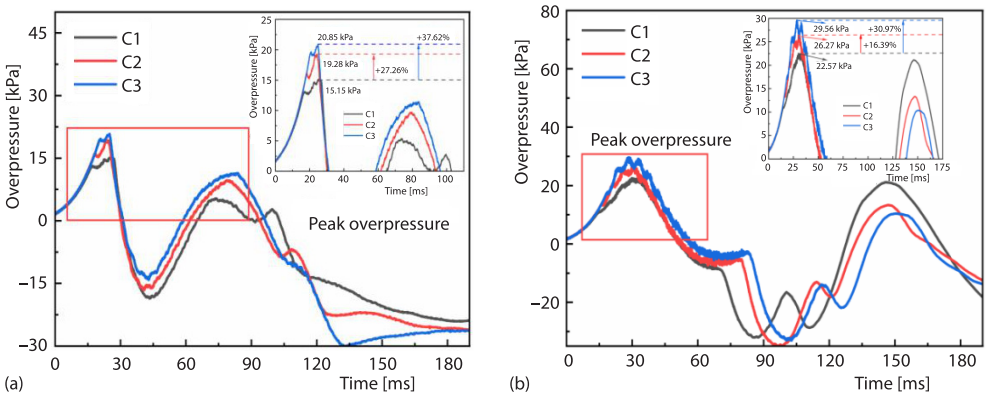

Figure 8. Dynamic changes of overpressure of CH_4/C_2H_6 mixture explosion in empty pipe-line; (a) upstream and (b) downstream

When φ = 10%, P1 peaks at 15.15 kPa and P2 peaks at 22.57 kPa. When φ = 20%, P1 peaks at 19.28 kPa and P2 peaks at 26.27 kPa, with upstream and downstream increases of 27.26% and 16.39%, respectively, compared to φ = 10%. When φ = 30%, P1 peaks at 20.85 kPa and P2 peaks at 29.56 kPa, an upstream and downstream increase of 37.62% and 30.97%, respectively, compared to φ = 10%. The P1 shows a trend of rising, then falling and rising again. The peak of overpressure occurs at about 25 ms, and the pressure begins to fall sharply after reaching the peak overpressure, P2 rises first and then fall, its slightly larger compared to P1, the peak overpressure time is about 30 ms, and it declines more slowly than P1 but with a more pronounced amplitude.

Figures 9-11 show the effect of nickel foam with different porosity on the explosion overpressure of CH_4/C_2H_6 mixtures while C_2H_6 volume fractions φ = 10%, 20%, and 30%, respectively. It can be seen that the effect of nickel foam with different porosity may lead to an increase or decrease in the peak explosion overpressure. In figs. 9-11, when the nickel foam quenching successfully, the upstream and downstream explosion overpressure change trend is approximately the same. There is only one peak value of upstream and downstream overpressure. When flame quenching failure, the explosive reaction intensifies, and the downstream peak overpressure is larger than the upstream. This indicates that the failure of flame quenching will increase the explosion overpressure. The reason is that the nickel foam fails to block the flame and its solid-phase structure acts as an obstacle, so the flame burns more vigorously, and the explosion overpressure is also increased. The phenomenon of wave peaks accompanied by

fluctuations in the overpressure graph is due to the repeated vibration of the pressure curve, resulting in the formation of multiple peaks. This phenomenon is mainly due to the membrane rupture during the propagation of the explosion shock wave, resulting in a significant decrease in the overpressure generated by the explosion. After pressure relief, the explosion overpressure exhibits oscillatory characteristics with enhanced turbulence intensity due to the increase of vortices. The first observation in the overpressure image is that the maximum overpressure peak of the premixed gas downstream in the pipe-line is maintained for a longer period compared to the maximum upstream pressure, and this peak is determined by the competition between multiple peaks [24, 25].

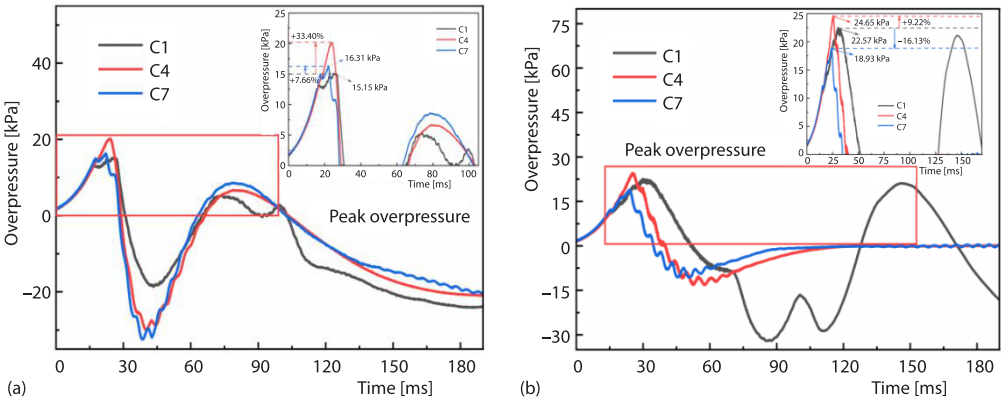

Figure 9. The φ = 10%, effect of foam nickel with different porosity on explosion overpressure of CH_4/C_2H_6 mixture; (a) upstream and (b) downstream

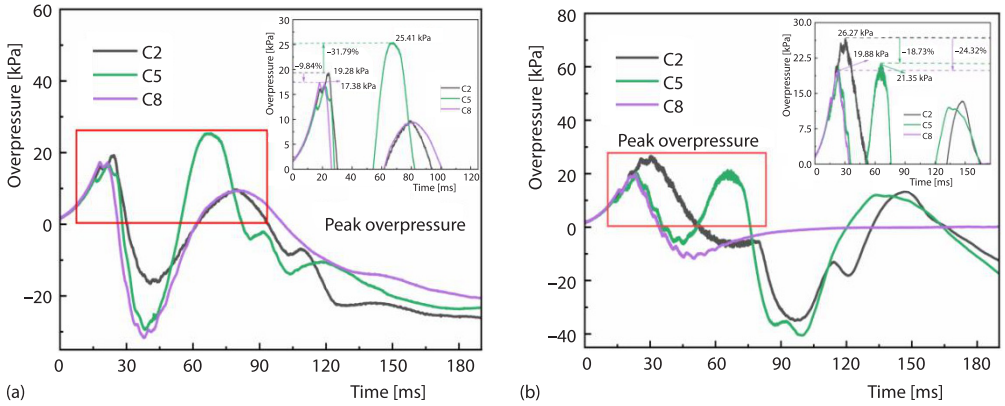

Figure 10. The φ = 20%, effect of foam nickel with different porosity on explosion overpressure of CH_4/C_2H_6 mixture; (a) upstream and (b) downstream

As shown in fig. 9, when the volume fraction of C_2H_6 is 10%, the upstream peak overpressure increases by 33.40% and 7.66% with the increases of the porosity of nickel foam, respectively, the downstream peak overpressure of 30 PPI nickel foam decreases by 16.13%, and the downstream peak overpressure of 40 PPI nickel foam increases by 9.22%. As shown in fig. 10, when the volume fraction of C_2H_6 is 20%, compared with the empty tube, the upstream peak overpressure of 30 PPI nickel foam increases by 31.79%, and the upstream peak overpressure of 40 PPI nickel foam decreases by 9.84%. With the increase in the porosity of nickel foam, the

downstream peak overpressure decreases by 18.73% and 24.32%, respectively. As can be seen in fig. 11, when the volume fraction of C_2H_6 is 30%, compared with the empty pipe, the upstream peak overpressure of 30 PPI nickel foam increases by 7.05%, the upstream peak overpressure of 40 PPI nickel foam decreases by 26.52%. With the increase in the porosity of the nickel foam, the downstream peak overpressure decreases by 8.29% and 47.56%, respectively.

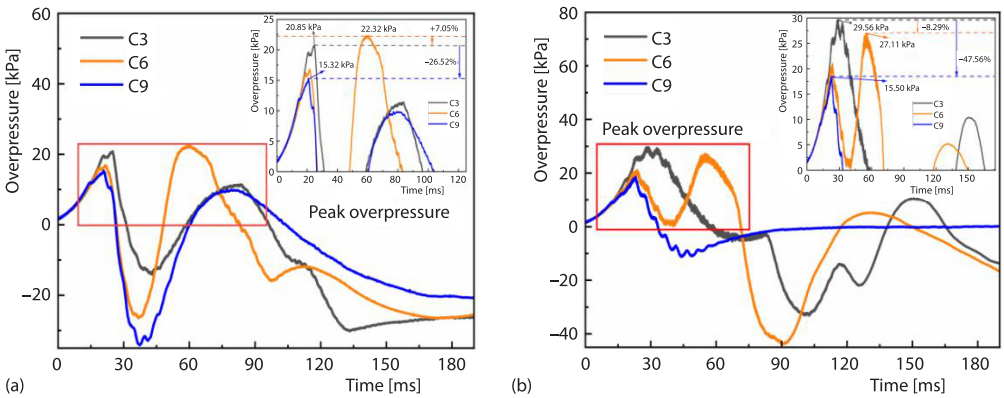

Figure 11. The φ = 30%,effect of foam nickel with different porosity on explosion overpressure of CH_4/C_2H_6 mixture; (a) upstream and (b) downstream

In summary, it can be concluded that the explosion overpressure is affected by the C_2H_6 volume fraction. Nickel foam's promotion or suppression depends on its porosity. When the flame is quenched, the porous material can effectively suppress the explosion overpressure and the suppression effect is weakened with the increase of the C_2H_6 volume fraction. When the flame quenching failure, the downstream explosion overpressure increases abruptly, and the upward tendency is strengthened with the increase of the C_2H_6 volume fraction.

Mechanism analysis

In this paper, the porous material is placed vertically in an explosion experimental pipe, and the primary investigation is focus on the quenching behavior of porous materials on flames [26]. According to the cold wall quenching mechanism of porous materials, when the flame is in contact with the porous material, its particular pore structure can shear and split the flame, resulting in multiple collisions between the flame and the internal pore structure of the porous increases the contact area with the pore wall, the porous material reduces the flame's temperature through heat transfer and energy absorption until it reaches the quenching temperature to extinguish the flame [27]. The pore structure of porous materials leads to an increase in the concentration of upstream premixed gases, which increases the frequency of free radicals colliding with the pore walls and reduces the number of free radicals effectively involved in the combustion reaction, which in turn inhibits the formation and propagation of flames [28]. In addition, the porous medium has a suppression effect on the blast shock wave. When the shock wave contacts the porous material, part of the energy of the shock wave will be dissipated by the reflection of the solid surface. The irregular pores inside the porous material will lead to the reflection and scattering of the shock wave, forming a reflected pressure wave, which further dissipates the energy [29]. These reflected pressure waves interfere with flame propagation, causing the flame structure to become dispersed and reducing the flame propagation velocity.

Combining the quenching and pressure decay mechanisms of porous materials mentioned previously, the mechanism of nickel foam on the flame propagation of CH_4/C_2H_6 mixture

explosion is explored. As can be seen from fig. 12, when the nickel foam porosity is 30 PPI, the explosion flame has the effect of both promoting and inhibiting, this is because the explosion intensity is related to the volume fraction of C_2H_6 in the gas mixture, the flame propagation speed and explosion overpressure with the volume fraction of C_2H_6 is proportional. When the explosion flame quenching fails, nickel foam as an obstacle to accelerate the flame spread, and the flame breaks through the porous nickel foam bondage ignited downstream gas, causing the secondary deflagration phenomenon. When the explosion flame quenching success, the flame cannot penetrate the nickel foam, nickel foam inhibits the flame propagation successfully. When the nickel foam porosity is 40 PPI, with the increase of nickel foam porosity, the nickel foam cold wall quenching effect is enhanced, and also the free radicals collision of the pore wall, which reduces the number of free radicals that are effectively involved in the combustion reaction, and inhibits the formation and propagation of the flame.

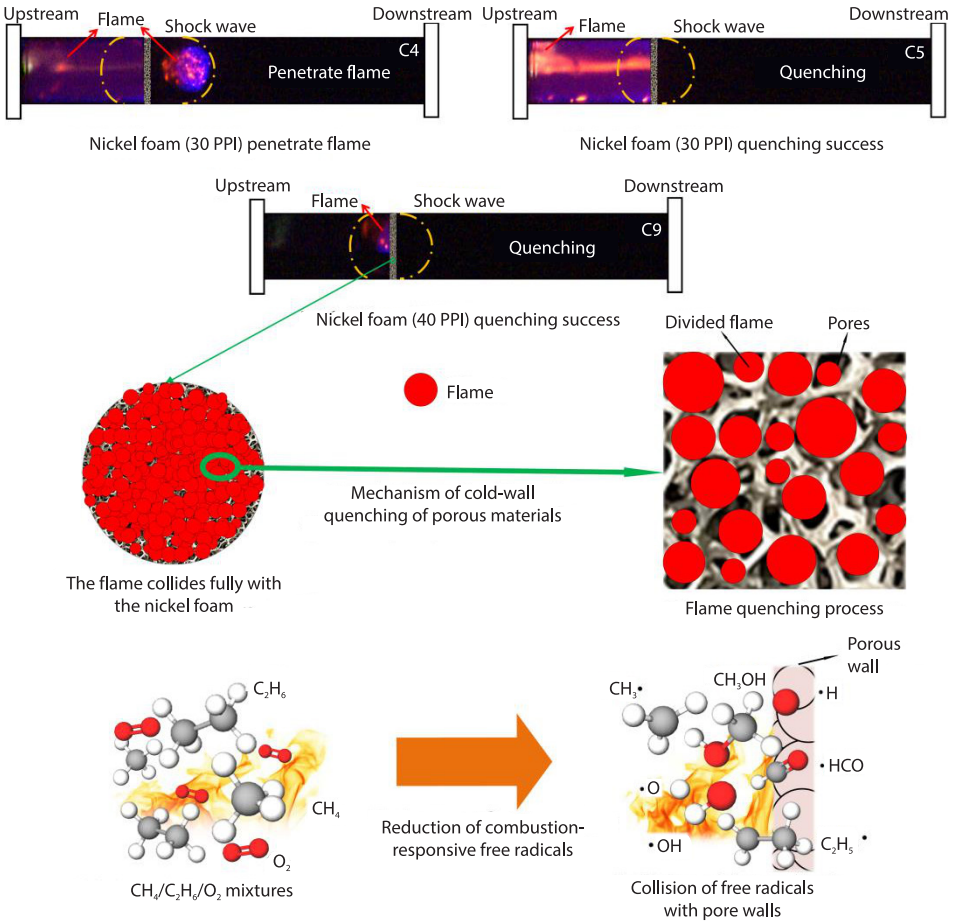

Figure 12. Mechanism of porous material effect on explosion flame propagation

Therefore, it can be concluded that nickel foam may have two different effects on the flame propagation of CH_4/C_2H_6 mixture explosion: quenching successful and quenching failure. Quenching failure will accelerate the flame propagation so that the explosion intensifies, nickel foam porosity of 30 PPI explosion suppression is limited, nickel foam porosity of 40 PPI

explosion suppression effect is significant, the explosion flame quenching successful. Larger porosity provides better safety protection for CH_4/C_2H_6 gas explosions.

Conclusions

This paper investigates the technology of nickel foam to suppress the explosion of CH_4/C_2H_6 mixtures and analyzes the explosion characteristics of CH_4/air-premixed gases. The main results are as follows.

- The nickel foam has two effects on the CH_4/C_2H_6 mixture: explosion flame promotion and inhibition. When quenching failure, the peak velocity and peak overpressure appeares in the second peak. When quenching successfully, the flame propagation is blocked, and the peak flame velocity and overpressure decreases, and the peak value of velocity and pressure appears in the first wave peak.
- Flame velocity and explosion overpressure changes is affected by C_2H_6 volume fraction. When the flame is quenched, the porous material can effectively inhibit the explosion overpressure and flame propagation speed. The inhibition effect weakened with the increase of C_2H_6 volume fraction. When the flame quenching fails, the explosion overpressure and flame propagation velocity increases abruptly.
- The porosity of porous materials has a significant impact on explosions. When the porosity is low, it may result in successful or failed explosion suppression. The probability of suppression successful increases with the increases of porosity of porous materials, larger porosity provides greater safety assurance.

Acknowledgment

This work was supported by the Science and Technology Research Program of Chongqing Municipal Education Commission (KJZD-K202401501); National Natural Science Foundation of China (52274177). Thanks.

References

[1] Sun, S., *et al*., Effects of Concentration and Initial Turbulence on The Vented Explosion Characteristics of Methane-Air Mixtures, *Fuel*, *267* (2020), 117103
[2] Erjiang, H., *et al*., Experimental Study on Ethane Ignition Delay Times and Evaluation of Chemical Kinetic Models, *Energy and Fuel, 29* (2015), 7, pp. 4557-4566
[3] Golovastov, S. V., *et al*., Evolution of Detonation Wave and Parameters of Its Attenuation when Passing along a Porous Coating, *Experimental Thermal and Fluid Science*, *100* (2019), Jan., pp. 124-134
[4] Su, B., *et al*., Coupling Analysis of the Flame Emission Spectra and Explosion Characteristics of CH_4/C_2H_6/Air Mixtures, *Energy & Fuel*s, *34* (2019), 1, pp. 920-928
[5] Luo, Z., *et al*., Experimental Study on the Deflagration Characteristics of Methane-Ethane Mixtures in a Closed Duct, *Fuel*, *259* (2020), 116295
[6] Duan, Y., *et al*., Experimental Study on Methane Explosion Characteristics with Different Types of Porous Media, *Journal of Loss Prevention in the Process Industries*, *69* (2021), 104370
[7] Cao, X., *et al.*, Experimental Research on the Characteristics of Methane/Air Explosion Affected by Ultrafine Water Mist, *Journal of Hazardous Materials*, *324* (2017), Part B, pp. 489-497
[8] Wang, L., *et al*., Synergistic Suppression Effects of Flame Retardant, Porous Minerals and Nitrogen on Premixed Methane/Air Explosion, *Journal of Loss Prevention in the Process Industries*, *67* (2020), 104263
[9] Yang, W., *et al*., Effect of Ignition Position and Inert Gas on Hydrogen/Air Explosions, *International Journal of Hydrogen Energy*, *46* (2021), 12, pp. 8820-8833
[10] Jianhua, S., *et al.*, The Comparative Experimental Study of the Porous Materials Suppressing the Gas Explosion, *Procedia Engineering*, *26* (2011), pp. 954-960
[11] Duan, Y., *et al.*, Exploration of Critical Hydrogen-Mixing Ratio of Quenching Methane/Hydrogen Mixture Deflagration under Effect of Porous Materials in Barrier Tube, *International Journal of Hydrogen Energy*, *48* (2023), 58, pp. 22288-22301

[12] Cui, Y. Y., *et al*., Effect of Wire Mesh on Double-Suppression of CH_4/Air Mixture Explosions in a Spherical Vessel Connected to Pipe-Lines, *Journal of Loss Prevention in the Process Industries*, *45* (2017), Jan., pp. 69-77
[13] Nie, B., *et al.*, The Roles of Foam Ceramics in Suppression of Gas Explosion Overpressure and Quenching of Flame Propagation, *Journal of Hazardous Material*s, *192* (2011), 2, pp. 741-747
[14] Pang, L., *et al.*, A Study on the Characteristics of the Deflagration of Hydrogen-Air Mixture under the Effect of a Mesh Aluminum Alloy, *Journal of Hazardous Materials*, *299* (2015), Dec., pp. 174-180
[15] Yulong, D., *et al.*, Characteristics of Gas Explosion Diffusion Combustion under Porous Materials, *Explosion and Shock Waves*, *40* (2020), 9, 095401
[16] Long, F., *et al*., Effect of Porous Materials on Explosion Characteristics of Low Ratio Hydrogen/Methane Mixture in Barrier Tube, *Journal of Loss Prevention in the Process Industries*, *80* (2022), 104875
[17] Wu, S., Experimental Study on the Suppression of Explosion Flame in Pipe-lines with Porous Materials (in Chinese) M. Sc. thesis, Chongqing University of Science and Technology, Chongqing, China, 2018
[18] Zhou, S., *et al*., Effects of Mesh Aluminum Alloy and Aluminum Velvet on The Explosion of H_2/air, CH_4/air and C_2H_2/Air Mixtures, *International Journal of Hydrogen Energy*, *46* (2021), 27, pp. 14871-14880
[19] Pei, B., *et al.*, Experimental Study on the Synergistic Inhibition Effect of Nitrogen and Ultrafine Water Mist on Gas Explosion in a Vented Duct, *Journal of Loss Prevention in the Process Industries*, *40* (2016), Mar., pp. 546-553
[20] Ibrahim, S. S., Masri, A. R., The Effects of Obstructions on Overpressure Resulting from Premixed Flame Deflagration, *Journal of Loss Prevention in the Process Industries*, *14* (2001), 3, pp. 213-221
[21] Hu, E., *et al.*, Experimental and Numerical Study on the Effect of Composition on Laminar Burning Velocities of H_2/CO/N_2/CO_2/Air Mixtures, *International Journal of Hydrogen Energy*, *37* (2012), 23, pp. 18509-18519
[22] Luo, Z., *et al*., Experimental Study on the Deflagration Characteristics of Methane-Ethane Mixtures in a Closed Duct, *Fuel*, *259* (2020), 116295
[23] Radulescu, M. I., Lee J. H. S., The Failure Mechanism of Gaseous Detonations: Experiments in Porous Wall Tubes, *Combustion & Flame*, *131* (2002), 1-2, pp. 29-46
[24] Ma, Q., *et al*. Effects of Hydrogen Addition on the Confined and Vented Explosion Behavior of Methane in Air, *Journal of Loss Prevention in the Process Industries*, *27* (2014), Jan., pp. 65-73
[25] Rocourt, X., *et al*., Vented Hydrogen-Air Deflagration in a Small Enclosed Volume, *International Journal of Hydrogen Energy*, *39* (2014), 35, pp. 20462-20466
[26] Heinrich, A., *et al*., Investigation of the Turbulent Near-Wall Flame Behavior for a Sidewall Quenching Burner by Means of a Large Eddy Simulation and Tabulated Chemistry, *Fluids*, *3* (2018), 3, 65
[27] Wang, M., *et al*., Effect of Metal Foam Mesh on Flame Propagation of Biomass-Derived Gas in a Half-Open Duct, *ACS Omega*, *5* (2020), 32, pp. 20643-20652
[28] Wang, L., *et al*., Synergistic Suppression Effects of Flame Retardant, Porous Minerals and Nitrogen on Premixed Methane/Air Explosion, *Journal of Loss Prevention in the Process Industries*, *67* (2020), 104263
[29] Chen, P., *et al.,* Effects of Metal Foam Meshes on Premixed Methane-Air Flame Propagation in the Closed Duct, *Journal of Loss Prevention in the Process Industries*, *47* (2017), May, pp. 22-28

Paper submitted: September 7, 2024
Paper revised: October 18, 2024
Paper accepted: October 20, 2024